Unusual mosaic image of the Si(111)-(7×7) surface coinciding with field emission resonance in scanning tunneling microscopy

Keisuke Sagisaka* and Daisuke Fujita

Advanced Nano Characterization Center, National Institute for Materials Science, 1-2-1 Sengen, Tsukuba, Ibaraki 305-0047, Japan and International Center for Materials Nanoarchitectonics, National Institute for Materials Science, 1-2-1 Sengen, Tsukuba, Ibaraki 305-0047, Japan

(Received 24 March 2008; published 1 May 2008)

Scanning tunneling microscopy in field emission mode (with atomic resolution) reveals an unfamiliar topographic image of a clean Si(111) surface, so-called mosaic patterns, within a narrow range of high sample bias, in contrast to the conventional (7×7) superstructure observed at low sample bias. The mosaic patterns are found to be associated with the configuration of displaced center adatoms and adatom vacancies, induced by energetic electron injection, within the faulted half of the unit cell. At higher sample bias, the configuration of the displaced adatoms and the vacancies in the faulted half of the unit cell affects the topographic contrast of adatoms in the adjoining unfaulted half of the unit cells. This effect is greatly enhanced, thereby producing the mosaic patterns, when the sample bias matches the energy of the first field emission resonance state (V_s = +5.0 V) generated in the vacuum gap between the tip and the surface.

DOI: 10.1103/PhysRevB.77.205301 PACS number(s): 68.37.Ef, 68.47.Fg, 73.20.At

Under the existence of a strong electric field, the vacuum gap between the tip and sample in a scanning tunneling microscope (STM) is described as a triangular potential well. At the well, field-emitted electrons form standing waves through multiple reflections, which lead to resonant states. This phenomenon, known as field emission resonance (FER), is observed as oscillation in a differential conductance (dI/dV) spectrum on various surfaces of metals,[1–6] semiconductors,[7–9] and insulators.[10,11] Up to now, FER has been utilized for studying electron interference in a thin film and a buried layer,[8] lifetime of image potential states,[3,4] variation of local work function,[4,6] and spin splitting of image states of a magnetic island.[5]

The conventional STM in tunneling mode usually requires a conductive surface. On the other hand, it has been shown that FER is applicable to insulating surfaces such as a diamond[10] and thin amorphous SiO_2 films.[11] On a diamond surface, FER plays a role in obtaining atomic scale resolution. Field emission mode thus has the potential to extend the application range of STM in surface characterization. Although a number of spectroscopic experiments have been done, the study of FER imaging on the atomic scale is limited.[8,10] To elevate this technique to the practical level, it is important to accumulate fundamental knowledge on FER imaging.

In this paper, we report the observation of a previously unreported STM image of a low temperature Si(111)-(7×7) surface observed by utilizing FER. When this surface is scanned with a sample bias above approximately +2.0 V at low temperature, the center silicon adatom is laterally displaced within a faulted half (FH) of the unit cell, which was first reported by Stipe *et al.*[15] Such displacement is excited by injection of tunneling electrons or field-emitted electrons from the STM tip. In conjunction with the lateral displacement of adatoms, the constant-current imaging shows mosaic patterns around V_s = +5.0 V, which corresponds to the first FER peak energy. This unfamiliar image of the Si(111)-(7×7) surface is highly associated with the configuration of the displaced adatoms and adatom vacancies.

The experiments were performed in an ultrahigh vacuum STM (base pressure: 3.0×10^{-9} Pa). The sample was cut from a phosphorus-doped *n*-type Si(111) wafer with a resistivity of 0.01 Ω cm. A clean surface was obtained by flash to 1300 K, followed by slow cooling to room temperature to create the (7×7) reconstruction surface. STM images were collected using tungsten tips at liquid-nitrogen temperature. Moreover, dI/dV spectra were acquired by using the lock-in technique under the closed feedback loop.

Figure 1(a) shows a typical dI/dV spectrum taken from the Si(111)-(7×7) surface over a wide range of sample bias. The spectrum is characterized by a pronounced oscillation in the field emission region. These peaks are assigned to the FER states, as observed in previous studies on the Si(111)-(7×7) surfaces.[7,9] The position and the intervals of the peaks are observed to slightly shift when different tips are used.[9] The first and second resonance peaks typically appear around V_s = +4.95 and +6.4 V, respectively, while the minima between them are situated around V_s = +5.7 V.

Figures 1(b)–1(e) are constant-current images of the Si(111)-(7×7) surface observed using different sample biases. The image observed at +1.0 V [Fig. 1(b)] shows a typical dimer-adatom-stacking (DAS) fault structure with (7×7) periodicity: One unit cell contains 12 adatoms and shares four corner holes with the neighboring unit cells. Raising the sample bias to +4.0 V [Fig. 1(c)] creates many adatom vacancies, which results in different image contrast from that at +1.0 V, as will be discussed later. When the sample bias is set to a value slightly higher than the first FER peak, an unusual image is observed [Fig. 1(d)]. This image, recorded at V_s = +5.06 V, loses the (7×7) symmetry but exhibits geometrical patterns so-called "mosaic." This kind of image is observed when the sample bias is around +5.0 V and the tunneling current is 1.0 nA or below. The corrugation of these patterns is half to one-third, compared to that of the image at V_s = +1.0 V. Interestingly, the mosaic patterns are made of networks of bright and dark contrasts, instead of the

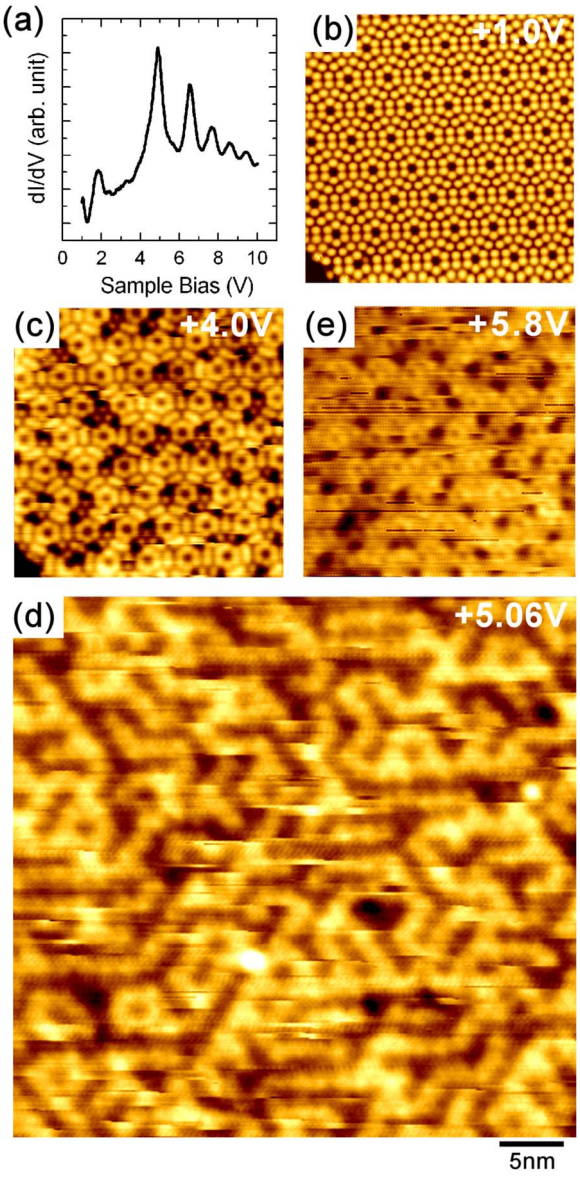

FIG. 1. (Color online) (a) dI/dV spectrum recorded on the Si(111)-(7×7) surface at 79 K (closed feedback loop, I_0=1.0 nA, modulation amplitude: 10 mV). [(b)–(e)] Constant-current images of the Si(111)-(7×7) surface at 79 K; I=0.2 nA. (b) V_s=+1.0, (c) +4.0, (d) +5.06, and (e) +5.8 V. Image size: [(b), (c), and (e)] 18×20 nm and (d) 90×100 nm.

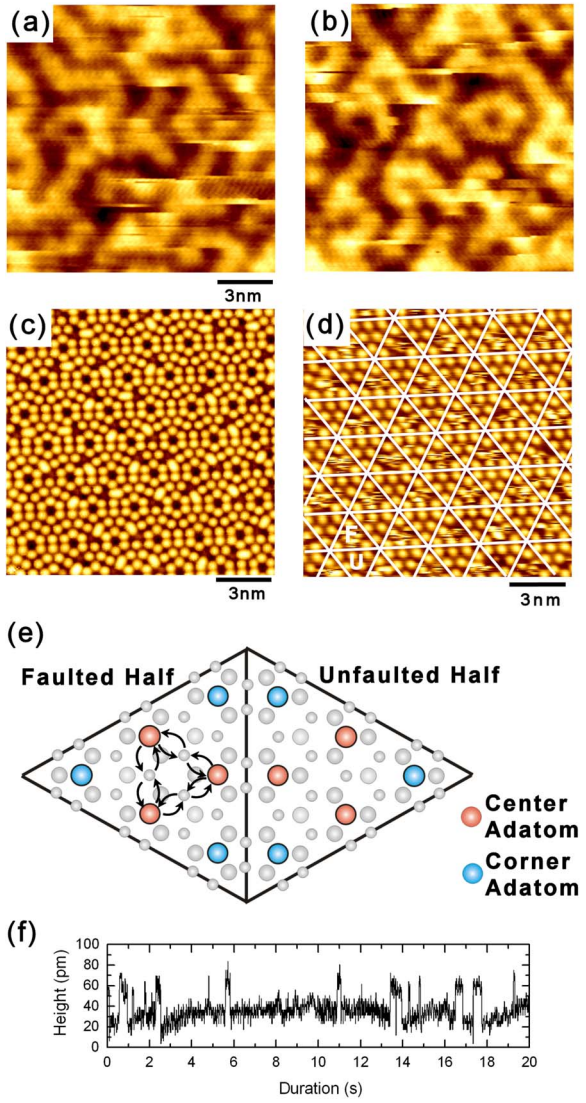

FIG. 2. (Color online) [(a) and (b)] Consecutive constant-current images of the Si(111)-(7×7) surface at 79 K; I=0.1 nA. (c) Constant-current image at V_s=+1.0 V in the same region as in (a) and (b). Image size: [(a)–(c)] 18×20 nm. (d) Constant-current image of the Si(111)-(7×7) surface at 79 K; V_s=+2.5 V and I=1.0 nA. Image size: 16×18 nm. (e) Schematic of the DAS structure model. (f) Z piezoheight recorded at V_s=+5.0 V and I=0.2 nA while the tip was fixed over a single center adatom in the FH of the unit cell. Variation between the two states is due to adatom displacement.

protrusions of individual adatoms. Actually, a careful inspection can find fine corrugations, which may be attributed to the individual atoms, inside the bright networks. Note that the formation of the mosaic patterns is not due to degraded image contrast with increasing the tip-sample separation, but it is most likely related to the effect of image enhancement by FER. In fact, as the first FER condition is passed, the mosaic patterns become invisible and the faint atomic contrast is retrieved [Fig. 1(e)].[16]

The configuration of the mosaic patterns varies while the surface is scanned. Figures 2(a) and 2(b) are consecutive frames recorded in the same region.[17] Even though they are consecutive, the two images reveal different patterns. Moreover, flickering noise is frequently observed along the scanning direction. The low-bias image in Fig. 2(c) is obtained immediately after the frame taken at +5.06 V. Many center adatoms are displaced in the FH of the unit cells and, accordingly, adatom vacancies are created. Since the initial surface has almost no defects before being scanned at V_s=+5.06 V, the displacement must have been caused by high-bias scans. These observations indicate that the displacement of the center adatoms plays a role in the formation of the mosaic patterns.

The Si(111)-(7×7) surface at low temperature manifests a phenomenon that the center adatoms hop from the original site of the DAS structure to one of the surrounding threefold

sites (T4 sites) and return to the original site while the surface is scanned with a sample bias greater than a certain threshold voltage. The schematic in Fig. 2(e) is the DAS model of the Si(111)-(7×7) surface that depicts the displacement of the center adatoms (red balls) between the normal site and the metastable site in the FH of the unit cell. This phenomenon was first investigated by Stipe *et al.*, who reported that at low temperature, i.e., below 175 K, the application of a positive voltage pulse greater than +2.0 V induces both a single adatom transfer and return within the half unit cell of the (7×7) structure, that the displacement of the adatoms is caused mostly in the FH, the probability of the displacement in the unfaulted half (UFH) is 100 times lower than in the FH, that the same process occurs while the surface is scanned at a high sample bias, and that the transfer rate and the return rate depend on the sample bias and current.[15]

Our observation on the Si(111)-(7×7) surface at 79 K is consistent with their observation. The threshold for adatom displacement in our sample is observed around +1.8 V. Figure 2(d) is an image recorded at V_s=+2.5 V, with a comparatively slower scanning speed of 14 nm/s to exaggerate the motion of the adatoms [cf. 225 nm/s for Figs. 2(a) and 2(b)]. The hopping of the center adatoms due to the high-bias scan is predominately observed in the FH. The displacement of the center adatom in the UFH is seldom seen and no corner adatoms are observed to move.

Stipe *et al.* suggested that the mechanism of the adatom displacement (both transfer and return) lies in the energetic electron injection from the STM tip and electron transport on the surface.[15] This excitation is thus not localized beneath the STM tip. On our samples, in fact, the adatom displacement induced by a pulse voltage of +5.0 V extends at least 60 nm away from the tip. The surface process hidden behind the mosaic image is therefore described as a constant displacement of the center adatoms between the normal and metastable sites and, consequently, as the creation and annihilation of the adatom vacancies. Under the imaging condition for Fig. 1(d), the center adatom tends to escape from the tip. The return rate is much lower than the transfer rate [Fig. 2(f)]. When the tunneling current is, however, beyond typically 1.0 nA, the mosaic patterns begin to deteriorate, because the hopping rate overwhelms the scanning speed of STM.

Figures 3(a) and 3(b) show a pair of dual-bias images of the Si(111)-(7×7) surface at V_s=+3.8 and +5.07 V. The dual-bias imaging with switching the bias at every pixel can directly correlate two images, although sequential imaging does not provide useful information, because the configuration of the adatoms changes every second during the high-bias scan. In the image taken at +3.8 V [Fig. 3(a)], the adatom displacement is observed in 97% of the FHs and in 5% of the UFHs in the scanned region. The magnified image in Fig. 3(c) shows that a single process of adatom transfer to one of the metastable sites results in an apparent pair of center adatoms (ellipse) and an adatom vacancy (gray circle) in the FH, shown in the center of the image. When the center adatom in the UFH (adatom A) is facing the paired adatom in the adjacent FH, its topographic contrast is enhanced. In contrast, when the center adatom in the UFH (adatom B) is facing the adatom vacancy in the adjacent FH, its topographic contrast is diminished. Moreover, this depressed adatom even has a different local electronic structure and local surface potential from those on the clean surface.[18]

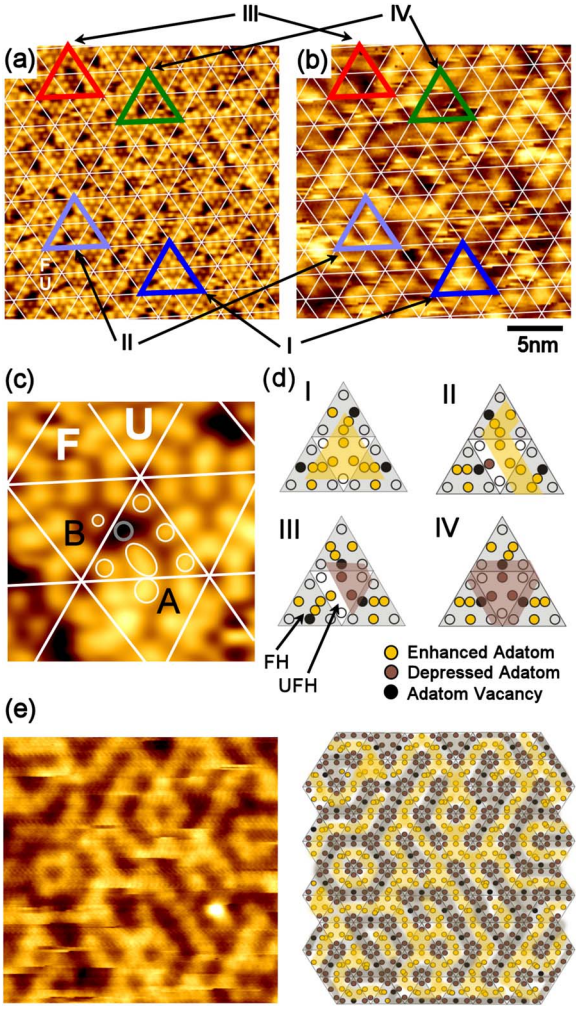

FIG. 3. (Color online) [(a) and (b)] Dual-bias images of the Si(111)-(7×7) surface at 79 K; (a) V_s=+3.8 and (b) +5.07 V; I=0.1 nA. Image size: 23×26 nm. (c) Magnified image of (a). Image size: 5×5.6 nm. Paired adatoms and adatom vacancy are marked with white ellipse and gray circle, respectively. The enhanced and diminished contrast of the center adatom in UFHs is represented by the size of the circles. (d) Schematics representing four types of adatom displacement found in (a) and (b). Bright adatoms, dark adatoms, and adatom vacancies for each situation found in (a) are shown in different colors/gray values. The patterns of enhancement by the FER found in (b) are emphasized in yellow/light gray and brown/dark gray. (e) Observed mosaic patterns (left) and schematic simulation (right), according to the rules of image enhancement found in (a) and (b).

The image at +5.07 V in Fig. 3(b) does not present mosaic patterns as clear as those in Fig. 1(d). This is due to the scan speed for recording images at two biases slower than the hopping rate of the adatoms. However, a comparison of two images in Figs. 3(a) and 3(b) still finds the following rules between the configuration of the adatoms and vacancies and the enhancement of image contrast by the FER.

(1) In the FH, the contrast of a center adatom and a paired adatom is enhanced, while an adatom vacancy gives rise to dark contrast.

(2) In the UFH, the contrast of a center adatom is enhanced when it is situated opposite an adatom or a paired adatom in the adjacent FH across the short diagonal of the unit cell [Fig. 3(d), I and II], while a center adatom results in dark contrast when it is situated opposite an adatom vacancy in the adjacent FH across the short diagonal of the unit cell [Fig. 3(d), III and IV].

(3) The contrast of the corner holes and the corner adatoms is depressed.

The third rule is also confirmed from the image obtained at around $V_s = +5.0$ V at room temperature, where only the center adatoms are imaged.[12] However, the mosaic image does not appear at room temperature, since the adatom displacement is not observed. In addition, the enhancement by the FER spatially exaggerates such characteristics, which produce the apparent networks of bright or dark contrast beyond the unit cells. To confirm the validity of the these rules, a mosaic image is schematically simulated. Following the rules, the mosaic patterns are completely duplicated in Fig. 3(e).

Finally, the mechanism by which the image of the Si(111)-(7×7) surface is enhanced is discussed in terms of the FER. The origin of the image contrast under the FER condition has been discussed in the cases of C-C dimer rows on a diamond surface[13] and a Moiré pattern in NaCl films grown on a silver surface.[14] The image contrast in both cases was attributed to the energy shift of the resonance peak between the sites producing bright and dark contrasts. Pivetta *et al.*[14] found that a modulation of the local work function caused the resonance-energy shift across the surface. Figure 4 shows site-dependent dI/dV spectra, including the first FER peak.[19] Our measurement resolves even a slight difference between the FER peaks, in terms of position and intensity, of the different sites in the unit cell of the (7×7) surface, which suggests that local surface potential variation exists even in a unit cell. The magnitude of the FER peak is most intense at the center adatom in the FH, while the other sites show weaker intensities. This observation is consistent with the fact that the mosaic patterns are the networks of enhanced contrast of the center adatoms across the surface, although the intensity for the center adatom in the UFH is weaker than expected. From the observation in Fig. 3, it is clear that the intensity of the FER peak at the center adatom in the UFH is easily influenced by the adatom configuration in the adjacent FH. The simultaneous topography shows that the center adatom in the FHs is mobile during spectroscopic measurement. We, therefore, speculate that the observed intensity at the center adatom in the UFH results from compensation of enhanced and depressed conductance, which lead to the weaker peak intensity than expected.

In summary, STM imaging with atomic resolution was performed on a Si(111)-(7×7) surface by using the field emission mode. This imaging found that adatom displacement under the application of a high sample bias gives rise to mosaic patterns in topography around $V_s = +5.0$ V. This bias

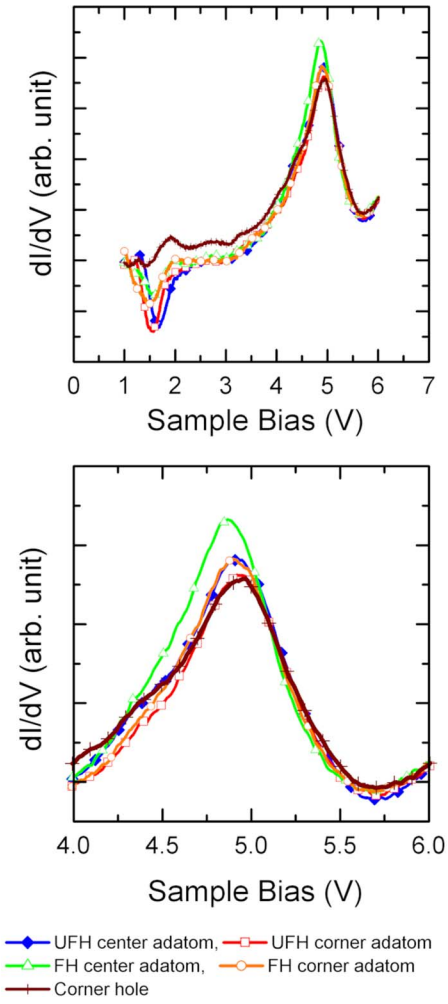

FIG. 4. (Color online) (Top) Site-dependent dI/dV spectra recorded from the Si(111)-(7×7) surface at 79 K (closed feedback loop, $I_0 = 1.0$ nA; modulation amplitude: 10 mV). (Bottom) Enlarged around +5.0 V.

corresponds to the energy of the first FER state generated in the vacuum gap between the tip and the surface. The mosaic patterns are found to result from the contrast enhancement through the FER, which produces a sort of network of the bright parts (in association with the enhanced center adatoms) and dark parts (in association with the depressed center adatoms, the adatom vacancies, and the corner adatoms). The mosaic patterns are observed on the Si(111)-(7×7) surface by coinciding several features, such as FER, a large unit cell of Si(111), adatom displacement within FH of the unit cell by energetic electron injection, and modification of local surface potential induced by the adatom displacement. We believe that the formation of the mosaic patterns caused by FER is unique to the Si(111)-(7×7) surface.

ACKNOWLEDGMENTS

This work was supported in part by World Premier International Research Center Initiative (WPI Initiative) on Materials Nanoarchitectonics, MEXT, Japan.

*sagisaka.keisuke@nims.go.jp

[1] G. Binnig, K. H. Frank, H. Fuchs, N. Garcia, B. Reihl, H. Rohrer, F. Salvan, and A. R. Williams, Phys. Rev. Lett. **55**, 991 (1985).
[2] T. Jung, Y. W. Mo, and F. J. Himpsel, Phys. Rev. Lett. **74**, 1641 (1995).
[3] P. Wahl, M. A. Schneider, L. Diekhoner, R. Vogelgesang, and K. Kern, Phys. Rev. Lett. **91**, 106802 (2003).
[4] J. I. Pascual, C. Corriol, G. Ceballos, I. Aldazabal, H.-P. Rust, K. Horn, J. M. Pitarke, P. M. Echenique, and A. Arnau, Phys. Rev. B **75**, 165326 (2007).
[5] A. Kubetzka, M. Bode, and R. Wiesendanger, Appl. Phys. Lett. **91**, 012508 (2007).
[6] C. L. Lin, S. M. Lu, W. B. Su, H. T. Shih, B. F. Wu, Y. D. Yao, C. S. Chang, and T. T. Tsong, Phys. Rev. Lett. **99**, 216103 (2007).
[7] R. S. Becker, J. A. Golovchenko, and B. S. Swartzentruber, Phys. Rev. Lett. **55**, 987 (1985).
[8] J. A. Kubby, Y. R. Wang, and W. J. Greene, Phys. Rev. Lett. **65**, 2165 (1990).
[9] Y. Suganuma and M. Tomitori, Jpn. J. Appl. Phys., Part 1 **39**, 3758 (2000).
[10] K. Bobrov, A. J. Mayne, and G. Dujardin, Nature (London) **413**, 616 (2001).
[11] K. Xue, H. P. Ho, J. B. Xu, and R. Z. Wang, Appl. Phys. Lett. **90**, 182108 (2007).
[12] J. A. Kubby, Y. R. Wang, and W. J. Greene, Phys. Rev. B **43**, 9346 (1991).
[13] K. Bobrov, L. Soukiassian, A. J. Mayne, G. Dujardin, and A. Hoffman, Phys. Rev. B **66**, 195403 (2002).
[14] M. Pivetta, F. Patthey, M. Stengel, A. Baldereschi, and W.-D. Schneider, Phys. Rev. B **72**, 115404 (2005).
[15] B. C. Stipe, M. A. Rezaei, and W. Ho, Phys. Rev. Lett. **79**, 4397 (1997).
[16] When the sample bias matches the second or third resonance state, similar mosaic patterns are observed again. However, the contrast of mosaic patterns is weaker than that of the first resonance state. Instead, a 7×7 lattice becomes more visible.
[17] See EPAPS Document No. E-PRBMDO-77-008820 for an electronic file representing the time evolution of the mosaic patterns. For more information on EPAPS, see http://www.aip.org/pubservs/epaps.html.
[18] The electronic structure of the depressed adatom will be discussed in a separate paper.
[19] The dI/dV spectra were collected at 128×128 locations over several unit cells during topographic imaging at +1.0 V. Each spectrum is obtained by averaging 16–24 spectra site by site (4–6 spectra from one adatom per unit cell are averaged over four unit cells).